PROCEEDINGS OF SCIENCE

Low Q^2 Spin Structure Results from Jefferson Lab

David Ruth[a,*]

[a] *University of New Hampshire,*
9 Library Way, Durham, NH, United States of America

E-mail: david.ruth@unh.edu

There is a pressing need for experimental measurements capable of testing chiral perturbation theory and other long distance effective theories. One of the most valuable quantities for performing low Q^2 comparisons between experiment and theory is that of the nucleon spin structure function. The spin structure functions g_1 and g_2 enable direct tests of effective theories of QCD through their moments, and a series of sum rules involving their integration. The Thomas Jefferson National Accelerator (JLab) in Newport News, VA, USA, has hosted a highly successful and ongoing program to measure these quantities over a broad kinematic range. In particular, the last few years have produced newly published JLab results measuring these spin structure functions at low Q^2 for both the proton and the neutron. In this proceedings, these recent low Q^2 spin structure results are summarized, along with prospects for future measurements.

The 11th International Workshop on Chiral Dynamics (CD2024)
26-30 August 2024
Ruhr University Bochum, Germany

*Speaker

 ISSN 1824-8039 . Published by SISSA Medialab.

PoS(CD2024)027

1. Introduction

Chiral effective theories are used to understand the long-distance regime of Quantum Chromodynamics (QCD), where perturbative QCD methods fail. But as these theories become increasingly developed, one pressing question is how to test them experimentally in the face of a dearth of observables which can be used for direct experimental tests of QCD. However, a few such observables exist, one of the most successful of which for testing low Q^2 effective theories are the spin structure functions g_1 and g_2. These structure functions, which can be extracted with inclusive electron scattering and a spin polarized nucleon target, can be integrated to form moments and spin polarizabilities which are directly computable with Chiral Perturbation Theory (χPT) and other effective theories. A program at the Thomas Jefferson National Accelerator Facility in Newport News, VA, USA has been highly successful at measuring these spin structure functions over a broad kinematic region for both the proton and neutron, culminating in an exciting set of published results over the last few years. In the following sections, these results and the experiments which produced them are presented and summarized.

To characterize the interaction rate and scattering cross section for an inclusive electron scattering interaction, it is necessary to write the leptonic and hadronic tensors in terms of the kinematic variables of the scattered electron. Here, the hadronic tensor consists of a symmetric part which contains unpolarized structure functions $W_1(\nu,Q^2)$ and $W_2(\nu,Q^2)$, and an antisymmetric part containing polarized structure functions $G_1(\nu,Q^2)$ and $G_2(\nu,Q^2)$, which only enters when the hadronic target is spin-polarized. These structure functions are written in terms of the electron's energy transfer ν and momentum transfer Q^2. This exercise is carried out in full in [1, 2], but for the purposes of this proceedings we focus on the extraction of the polarized structure functions of the nucleon. The full form of the cross section $\sigma = \frac{d\sigma}{dEd\Omega}$ is dependent on the angle of the hadron spin polarization vector $\vec{S}$ and the electron spin vector $\vec{s}$, as well as the scattering angle of the electrons θ.

To isolate the polarized structure functions, we take the difference between the cross section where the electron spin has forward helicity and the one where the electron spin has backward helicity, cancelling the terms associated with the symmetric part of the hadronic tensor. We can write two variants on this cross section difference, depending on whether the hadron polarized is aligned in the same direction as the incident electron beam, or transverse to it:

$$\Delta\sigma_{\parallel} = \frac{d^2\sigma^{\uparrow\Uparrow}}{dE'd\Omega} - \frac{d^2\sigma^{\downarrow\Uparrow}}{dE'd\Omega} = \left(\frac{d\sigma}{d\Omega}\right)_{Mott} \frac{4E^2}{Q^2}\tan^2\frac{\theta}{2}\sin^2\frac{\theta}{2}\times \left(MG_1(\nu,Q^2)\left[E+E'\cos\theta\right] - Q^2G_2(\nu,Q^2)\right) \tag{1}$$

$$\Delta\sigma_{\perp} = \frac{d^2\sigma^{\uparrow\Rightarrow}}{dE'd\Omega} - \frac{d^2\sigma^{\downarrow\Rightarrow}}{dE'd\Omega} = \left(\frac{d\sigma}{d\Omega}\right)_{Mott} \frac{4E^2}{Q^2}\tan^2\frac{\theta}{2}\sin^2\frac{\theta}{2}\times E'\sin\theta\cos(\theta_{OoP})\left(MG_1(\nu,Q^2) + 2EG_2(\nu,Q^2)\right) \tag{2}$$

For these polarized cross section differences, $\uparrow\downarrow$ represents the spin of the electron and $\Uparrow\Rightarrow$ represents the spin of the hadron. E and E' represent the electron energy before and after scattering, respectively. θ_{OoP} is the out-of-plane scattering angle of the electron, and M is the mass of the

nucleon. $\left(\frac{d\sigma}{d\Omega}\right)_{Mott}$ is the Mott cross section for a point particle, allowing us to understand the structure functions as a description of a nucleon's spin-dependent deviation from pointlike behavior.

Notable $G_{1,2}$ are dimensionful quantities, so it is customary to instead write the cross section differences in terms of dimensionless structure functions $g_{1,2}$, where:

$$g_1(x, Q^2) = \nu M^2 G_1(\nu, Q^2) \tag{3}$$

$$g_2(x, Q^2) = \nu^2 M G_2(\nu, Q^2) \tag{4}$$

Such that:

$$\Delta\sigma_{\parallel} = \frac{d^2\sigma^{\uparrow\Uparrow}}{dE'd\Omega} - \frac{d^2\sigma^{\downarrow\Uparrow}}{dE'd\Omega} = \left(\frac{d\sigma}{d\Omega}\right)_{Mott} \frac{4E^2}{Q^2}\tan^2\frac{\theta}{2}\sin^2\frac{\theta}{2}\times \frac{1}{M_p}\left(\frac{1}{\nu}g_1(x, Q^2)\left[E + E'\cos\theta\right] - \frac{Q^2}{\nu^2}g_2(x, Q^2)\right) \tag{5}$$

$$\Delta\sigma_{\perp} = \frac{d^2\sigma^{\uparrow\Rightarrow}}{dE'd\Omega} - \frac{d^2\sigma^{\downarrow\Rightarrow}}{dE'd\Omega} = \left(\frac{d\sigma}{d\Omega}\right)_{Mott} \frac{4E^2}{Q^2}\tan^2\frac{\theta}{2}\sin^2\frac{\theta}{2}\times \frac{E'}{M_p}\sin\theta\cos\theta_{OoP}\left(\frac{1}{\nu}g_1(x, Q^2) + 2\frac{E}{\nu^2}g_2(x, Q^2)\right) \tag{6}$$

With two equations and two unknowns, it is clear that an extraction of g_1 and g_2 can be performed with a quality measurement of the polarized cross section differences $\Delta\sigma_{\parallel}$ and $\Delta\sigma_{\perp}$. The former is dominated by the spin structure function g_1 while the latter is dominated by g_2. Consequently, a measurement of g_1 largely relies on a parallel polarized target while a measurement of g_2 largely requires a transversely polarized one.

g_1 and g_2 are useful observables to study in large part because of kinematically weighted integrals of these quantities, known as moments or sum rules, which are calculable with virtual-virtual Compton Scattering (VVCS) cross sections, and can be computed directly by theoretical QCD frameworks. Using the Cauchy Integral Formula [3], we can write the a dispersion relation for the VVCS interference amplitudes as:

$$f_{TT}(\nu, Q^2) = \frac{1}{2\pi^2}\int_{\nu_\pi}^{\infty} \frac{K\nu\sigma_{TT}(\nu, Q^2)}{\nu'^2 - \nu^2}d\nu' \tag{7}$$

$$f_{LT}(\nu, Q^2) = \frac{1}{2\pi^2}\int_{\nu_\pi}^{\infty} \frac{K\nu'\sigma_{LT}(\nu, Q^2)}{\nu'^2 - \nu^2}d\nu' \tag{8}$$

Here ν_π is the pion production threshold and σ_{TT} and σ_{LT} are the virtual photon cross sections. These are related to the spin structure functions by [4]:

$$\{\sigma_{TT}, \sigma_{LT}\} = \frac{4\pi^2\alpha^2}{M_p K}\{g_1 - \frac{Q^2}{\nu^2}g_2, \frac{Q}{\nu}(g_1 + g_2)\} \tag{9}$$

We can perform an low-energy expansion on the dispersion relations where $\nu \ll \nu_\pi$ to obtain [4]:

$$\text{Re } f_{TT}(\nu, Q^2) = \frac{2\alpha}{M_p^2} I_A(Q^2)\nu + \gamma_0(Q^2)\nu^3 + O(\nu^5)... \tag{10}$$

$$\text{Re } f_{LT}(\nu, Q^2) = \frac{2\alpha}{M_p^2} Q I_{LT}(Q^2) + Q\delta_{LT}(Q^2)\nu^2 + O(\nu^4)... \tag{11}$$

The terms of these expansions are the first class of spin structure functions moments. Comparison to the Cauchy integrals and the relationship with structure functions g_1 and g_2 yields sum rules for these terms as a function of the spin structure functions. The first moment in the f_{TT} low-energy expansion (LEX) is:

$$I_A(Q^2) = \frac{2M_p^2}{Q^2} \int_0^{x_{PP}} \left(g_1(x, Q^2) - \frac{4M^2x^2}{Q^2} g_2(x, Q^2) \right) dx \tag{12}$$

This important integral is referred to as the GDH Sum Rule. At the real photon point, $Q^2 = 0$, the GDH Sum Rule is a function of the magnetic moment κ of the proton, such that:

$$I_A(0) = -\frac{2\pi^2\alpha\kappa^2}{M_p^2} \tag{13}$$

The second term in f_{TT}'s expansion is known as the generalized forward spin polarizability:

$$\gamma_0(Q^2) = \frac{16\alpha M_p^2}{Q^6} \int_0^{x_{PP}} x^2 \left(g_1(x, Q^2) - \frac{4M^2x^2}{Q^2} g_2(x, Q^2) \right) dx \tag{14}$$

Spin polarizabilities such as this describe a spin-dependent response of the nucleon to an external field. The integrals for I_A and γ_0 are dominated by the g_1 term due to the kinematic weighting. This means that an extraction of these moments requires, primarily, an extraction of g_1, or in other words, an experiment with a longitudinally polarized target.

Another spin polarizability of interest in these proceedings is the second term of the f_{LT} expansion, known as the longitudinal-transverse spin polarizability [5]:

$$\delta_{LT}(Q^2) = \frac{16\alpha M_p^2}{Q^6} \int_0^{x_{PP}} x^2 \left(g_1(x, Q^2) + g_2(x, Q^2) \right) dx \tag{15}$$

δ_{LT} was considered a benchmark test of χPT and other effective theories due to its expected insensitivity to the Δ-resonance. As will be shown in section 2, the experimental data for δ_{LT} has produced puzzling discrepancies from theoretical calculations at especially low Q^2.

We can also cast our previously introduced VVCS interference amplitudes into a covariant form:

$$S_1(\nu, Q^2) = \frac{\nu M_p}{\nu^2 + Q^2} \left(f_{TT}(\nu, Q^2) + \frac{Q}{\nu} f_{LT}(\nu, Q^2) \right) \tag{16}$$

$$S_2(\nu, Q^2) = -\frac{M_p^2}{\nu^2 + Q^2} \left(f_{TT}(\nu, Q^2) - \frac{\nu}{Q} f_{LT}(\nu, Q^2) \right) \tag{17}$$

We can write dispersion relations for S_1, S_2 and νS_2:

$$S_1(\nu, Q^2) = \frac{2}{\pi} \int_{\nu_{pp}}^{\infty} \frac{\nu' \, \text{Im} \, S_1}{\nu'^2 - \nu^2} d\nu' \tag{18}$$

$$S_2(\nu, Q^2) = \frac{2}{\pi}\int_{\nu_{pp}}^{\infty} \frac{\nu \,\mathrm{Im}\, S_2}{\nu'^2 - \nu^2} d\nu' \tag{19}$$

$$\nu S_2(\nu, Q^2) = \frac{2}{\pi}\int_{\nu_{pp}}^{\infty} \frac{\nu' \,\mathrm{Im}\, S_2}{\nu'^2 - \nu^2} d\nu' \tag{20}$$

Subtracting the latter two dispersion relations and exploiting the connection to $g_{1,2}$ yields an important "super-convergence" relation [6]:

$$\Gamma_2(Q^2) = \int_0^1 g_2(x, Q^2) dx = 0 \tag{21}$$

This integral, known as the Burkhardt-Cottingham Sum Rule, predicts that g_2 integrated across the full bjorken-x spectrum must vanish for all Q^2.

We can also perform a low energy expansion on the S_1 dispersion relation, yielding several moments which were discussed above, as well as one new one, the first moment of g_1:

$$\Gamma_1(Q^2) = \int_0^1 g_1(x, Q^2) dx \tag{22}$$

One final moment of interest to us here is extracted by using the Operator Product Expansion (OPE) on the generalized form of the VVCS forward Compton scattering amplitude at high Q^2. The full exercise of calculating the matrix elements of the forward scattering amplitude and using dispersion relations to link the matrix elements to the structure functions g_1 and g_2 is carried out in [7], with the end result of:

$$\int_0^1 x^n g_1(x, Q^2) = \frac{1}{4} a_n(Q^2); n = 0, 2, 4 \tag{23}$$

$$\int_0^1 x^n g_2(x, Q^2) = \frac{1}{4}\frac{n}{n+1}\big(d_n - a_n\big); n = 2, 4 \tag{24}$$

Here, a_n and d_n are the matrix elements of the forward scattering Compton amplitude. The n=0 case of the second relation is ignored because the OPE assumes implicitly that the B.C. sum rule previously introduced holds. Of interest to us is the matrix element d_2. For the n=2 case, we solve the previous two equations to obtain:

$$d_2(Q^2) = \int_0^1 x^2 \Big(2g_1(x, Q^2) + 3g_2(x, Q^2)\Big) dx \tag{25}$$

At high Q^2, this matrix element is identified as a color polarizability, which quantifies a color-dependent response to an external field. At lower Q^2, we can still employ this sum rule to look at the inelastic part:

$$\overline{d}_2(Q^2) = \int_0^{x_{pp}} x^2 \Big(2g_1(x, Q^2) + 3g_2(x, Q^2)\Big) dx \tag{26}$$

In the following sections, the newest experimental results for g_1 and g_2 are discussed, along with, especially, extractions of Γ_1, Γ_2, γ_0, I_A, δ_{LT}, and $\overline{d}_2$. These spin structure results were obtained at Jefferson Lab (JLab), a high-intensity electron linear accelerator in Newport News, VA. At JLab, traditional electron scattering measurements with a fixed target are collected across three experimental halls A, B, and C, where halls A and C utilize high resolution spectrometers, and hall B uses a large acceptance detector known as CLAS. The results below include data from all three experimental halls.

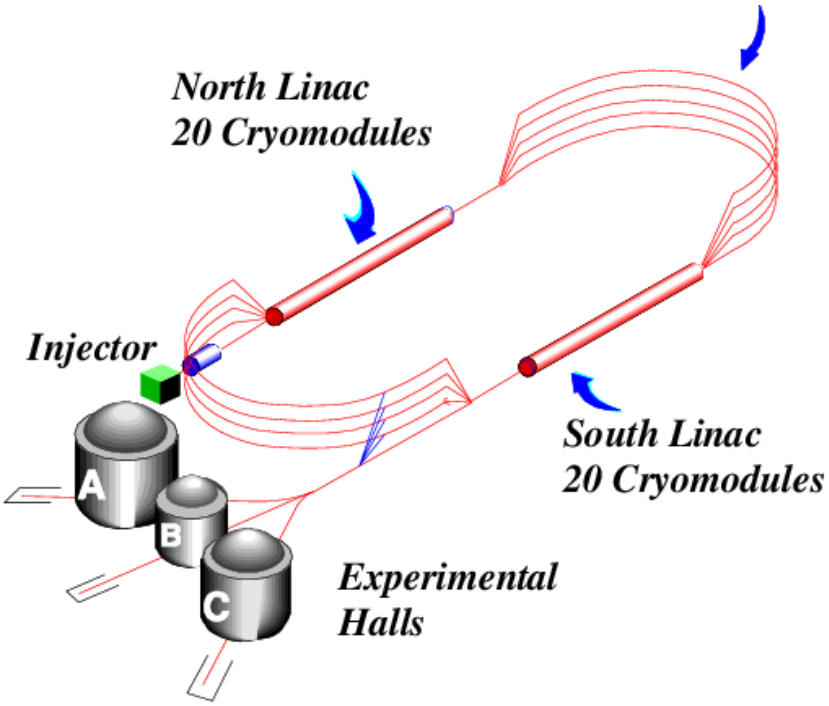

Figure 1: Jefferson Lab accelerator layout

2. Experimental Results

Though the experiments discussed in this proceedings have a number of variations in the specifics of detectors, equipment, and analysis method, the basic experimental setup and procedure is similar. Jefferson Lab consists of an electron beam which can reach energies between 1.1 GeV and 12 GeV, though at the time that most of the experiments discussed here ran the maximum beam energy was 6 GeV before a recent upgrade. The beam energy is achieved with two parallel linear accelerators, connected by recirculating arcs to create a 'racetrack' design, as in Figure 1. The beam electrons have a spin polarization which is rapidly flipped between alignment and antialignment with the beam direction to provide electrons of both needed helicities. Though higher beam current is achievable at JLab, the beam current for these experiments is limited to <100 nA to avoid depolarizing effects [8].

All of the experiments feature a polarized target. For experiments measuring the spin structure of the proton, this is generally solid ammonia (NH_3) polarized by means of Dynamic Nuclear Polarization (DNP) [9]. For the experiments measuring the neutron's spin structure, since a stable neutron target is not easily achievable, the standard target is polarized ^{3}He, which is polarized by spin-exchange optical pumping (seOP), and then utilized with analysis methods which attempt to isolate the neutron's contribution from that of the overall helium nucleus.

Though there are variations in the analysis procedure for each experiment, detailed in the relevant publications cited below, the general analysis procedure consists of measurements of counts of the forward and backward helicity scattered electrons, which are used to generate polarized asym-

metries, one for a parallel polarized target and one for a transversely polarized target:

$$A_{\parallel} = \frac{\sigma^{\uparrow\Uparrow} - \sigma^{\downarrow\Uparrow}}{\sigma^{\uparrow\Uparrow} + \sigma^{\downarrow\Uparrow}} \tag{27}$$

$$A_{\perp} = \frac{\sigma^{\uparrow\Rightarrow} - \sigma^{\downarrow\Rightarrow}}{\sigma^{\uparrow\Rightarrow} + \sigma^{\downarrow\Rightarrow}} \tag{28}$$

These asymmetries can be combined with the standard unpolarized cross section σ_0 to form the polarized cross sections differences of Eqs. 5 and 6:

$$\Delta\sigma_{\perp} = 2A_{\perp}\sigma_0 \tag{29}$$

$$\Delta\sigma_{\parallel} = 2A_{\parallel}\sigma_0 \tag{30}$$

The benefit of using this method is that there is significantly more unpolarized world data than polarized, so the models [10] for the unpolarized cross section σ_0 have become increasingly reliable [1]. We can then extract g_1 and g_2 from the polarized cross section differences, and calculate their moments with the sum rules of Section 1.

2.1 E94010

E94010 was one of the first measurements of nucleon spin structure at Jefferson Lab, collecting polarized neutron data in 1998 and publishing its first results in 2004. The experiment ran in Hall A, and used a polarized ^{3}He target, measuring scattering electrons with Hall A's High Resolution Spectrometers (HRS). This experiment was the first look at intermediate-to-low Q^2 g_1 and g_2 for the neutron, measuring both structure functions between a Q^2 of 0.3 - 1.0 GeV^2.

The published E94010 results [11] for the spin structure function moments are shown in Figure 2. Perhaps the most transformative result of the experiment comes in the surprising result for δ_{LT}; despite this quantity being a benchmark test for χPT, the E94010 results demonstrated a large tension at low Q^2 with the best available χPT calculation of Bernard et al., a discrepancy which some have referred to as the "δ_{LT} Puzzle". Γ_1 and Γ_2 show more expected behaviour: Γ_2 shows no sign of a B.C. sum rule violation, while Γ_1 results at low Q^2 seem to be converging both to the GDH Slope, as well as the Bernard et al. χPT calculation.

2.2 EG1b

With the results from E94010 filling in the first low Q^2 data for the neutron, it is natural to ask about intermediate-to-low Q^2 data for the proton. One major early experiment measuring the spin structure functions of the proton was known as EG1b, and ran in Hall B from 2000-2001 using the CLAS detector. As mentioned previously, the CLAS detector is a large acceptance spectrometer based on a six coil toroidal superconducting magnet.

The data collected in EG1b [12] was from a target polarized longitudinally with respect to the incident beam, and consequently, resulted in a high resolution measurement of the g_1 structure function of the proton, shown in figure 3. These results vary in Q^2 from around 0.04 - 5.4 GeV^2. Though no transverse data was collected, g_2 results were generated for the purposes of extracting the moments using the Wandzura-Wilczek relation [13]:

$$g_2^{WW}(x, Q^2) = \int_x^1 \frac{1}{y} g_1(y, Q^2) dy - g_1(x, Q^2) \tag{31}$$

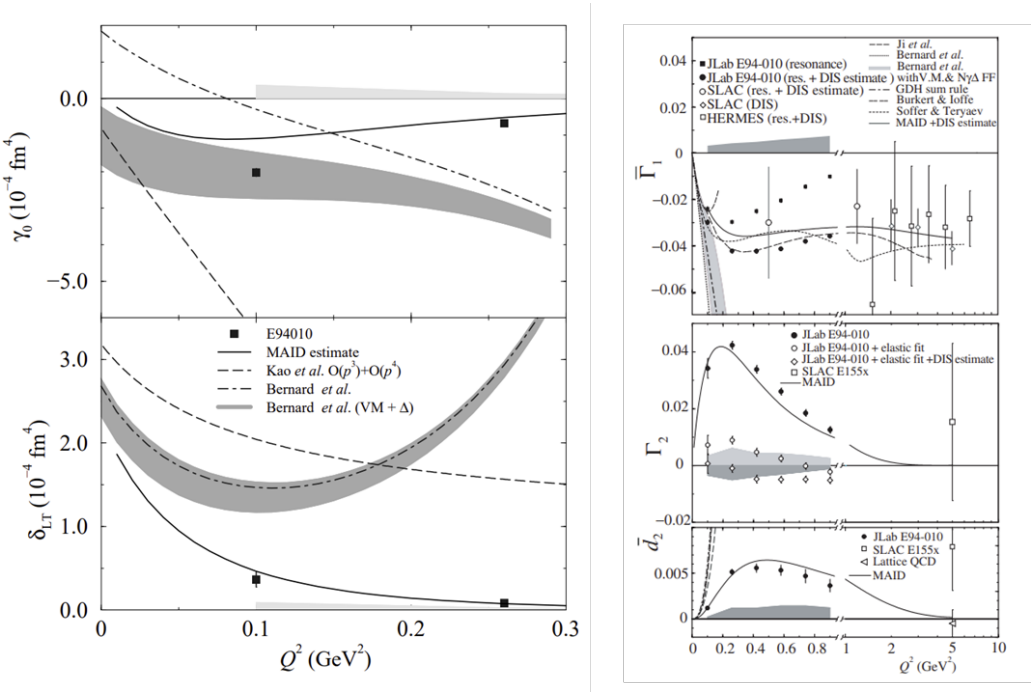

Figure 2: Moment results from E94010 for the neutron, for δ_{LT} and γ_0 (left) and Γ_1, Γ_2, and $\bar{d}_2$ (right) [11]

This relation relies on the assumption of leading twist (twist-2), so at lower Q^2s where higher twists contribute and the twist approximation eventually fails, the accuracy of g_2^{WW} is unknown.

Moment results from EG1b are shown in figure 4. Though the Γ_1 results again approach the χPT calculation and the GDH slope, we note a large discrepancy in the γ_0 plot between the two leading calculations, where the EG1b data seems to favor the Lensky calculation. However, the Bernard et al. calculation represents only the leading-order predictions and the subleading contributions are large, so a true comparison between the two calculations is not simple.

2.3 E97-110

Especially given the "δ_{LT}" puzzle of the first set of neutron data discussed above, it was highly necessary to collect more neutron data at even lower Q^2. The E97-110 experiment ran in Hall A in 2003, and published its results in *Nature Physics* in 2021 [14], becoming the first publication in a set of three in that journal covering the new spin structure results from Jefferson Lab. By this point, the χPT calculations had been refined and were in much better agreement with the previous neutron results. E97-110 (or, the "small-angle GDH experiment") used seOP with a ^{3}He target polarized both longitudinally and transversely to obtain g_1 and g_2 data for the neutron. Due to the use of a septum magnet enabling very small scattering angles as low as 6^circ with the Hall A High-Resolution Spectrometers (HRS), the experiment was able to measure almost an order of magnitude lower in Q^2 than its predecessor, E94010.

The results of E97-110 are shown in Figure 5 for the spin structure functions, and Figure 6 for the moments. The results for I are notable in that the experimental data agrees well with the Lensky et al. calculation at high Q^2, and crosses to better agreement with the Bernard et al. calculation

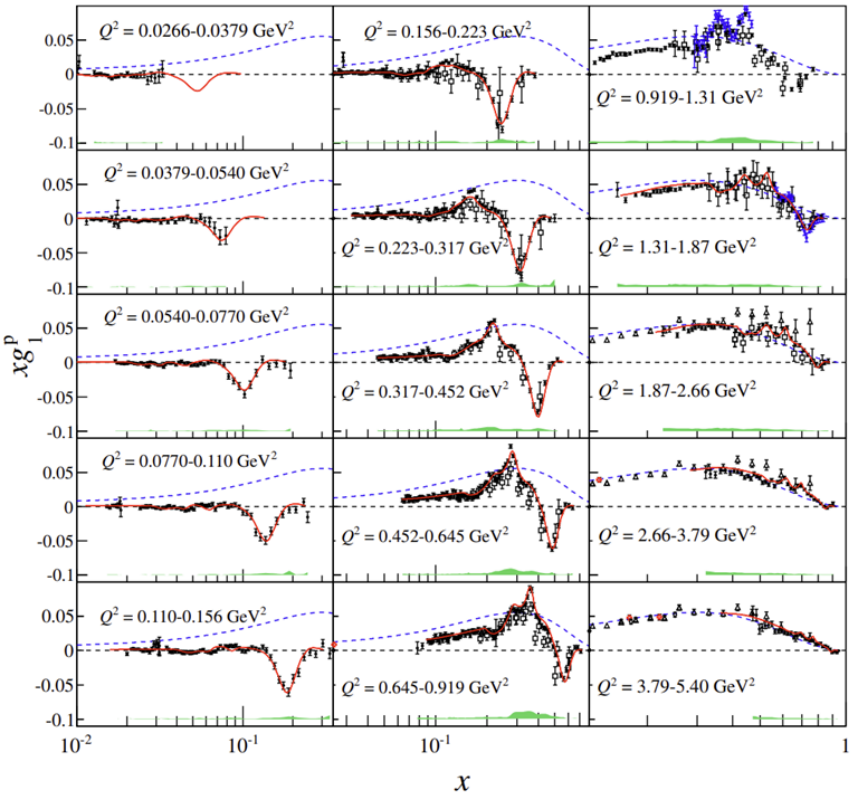

Figure 3: g_1 results for the proton from the EG1b experiment. [12]

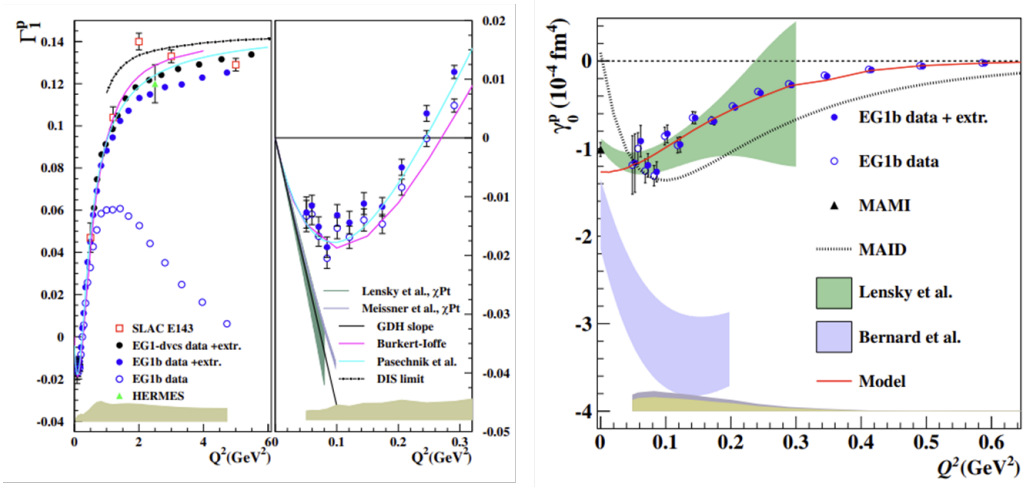

Figure 4: Moment results for the proton from the EG1b experiment for Γ_1 (left) and γ_0 (right).

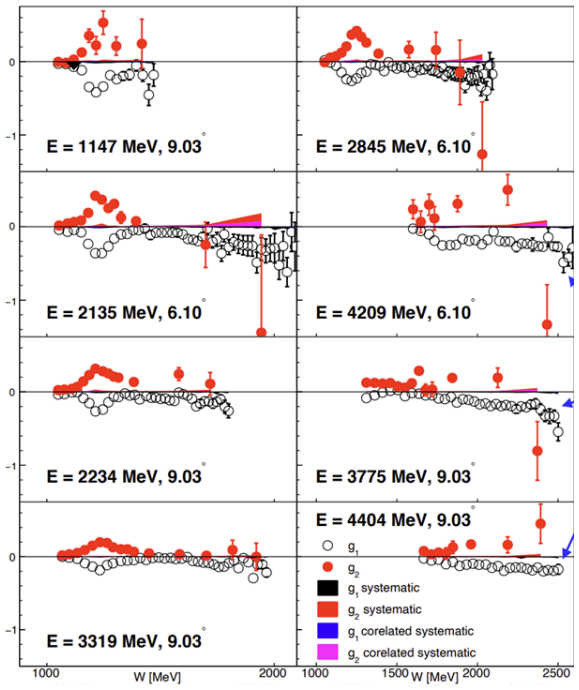

Figure 5: E97-110 results for g_1 and g_2 of the neutron [14]

at low Q^2. The spin polarizabilities present an even more puzzling disagreement: though both calculations now agree well with data in the Q^2 regime of E94010, the new, lower Q^2 data from E97-110 shows an increasingly large discrepancy from the χPT calculations for both δ_{LT} *and* γ_0, seemingly proving the "δ_{LT} Puzzle" to be alive and well. As of this writing the question of this deviation from chiral perturbation theory remains an open question.

2.4 E08-027

With E97-110 filling in neutron data down to a Q^2 of almost 10^{-2}, it is important to also investigate the spin structure of the proton in the same very low Q^2 regime. The two complementary final experiments discussed here do exactly that. E08-027, or the 'g2p experiment' collected data in 2012 Hall A with the HRS and a transversely polarized target, as well as a septum magnet enabling the collection of very small angle, and consequently very low Q^2 data from 0.02 - 0.13 GeV^2. In 2022 this experiment also published its first results in *Nature Physics* [15]. The experiment primarily focused on transverse data, and consequently, the extraction of the g_2 structure function, but also included one longitudinal setting and a matching extraction of g_1.

The structure function results of E08-027 are shown in Figure 7, and the moment results in Figure 8. The Γ_2 results cannot directly test the B.C. sum rule; higher Q^2 results use the assumption of leading twist and the g_2^{WW} of equation 31 to calculate the needed low-x part of the integral, but at the Q^2 of E08-027, the twist approximation has failed and there is no known way to estimate the low-x part. Assuming B.C. sum rule fulfillment however enables the difference between the full result and a Γ_2 of zero to be understood as an estimate of the magnitude of the low-x part of the integral. For δ_{LT}, the data show no sign of a δ_{LT} puzzle for the proton, largely agreeing well with

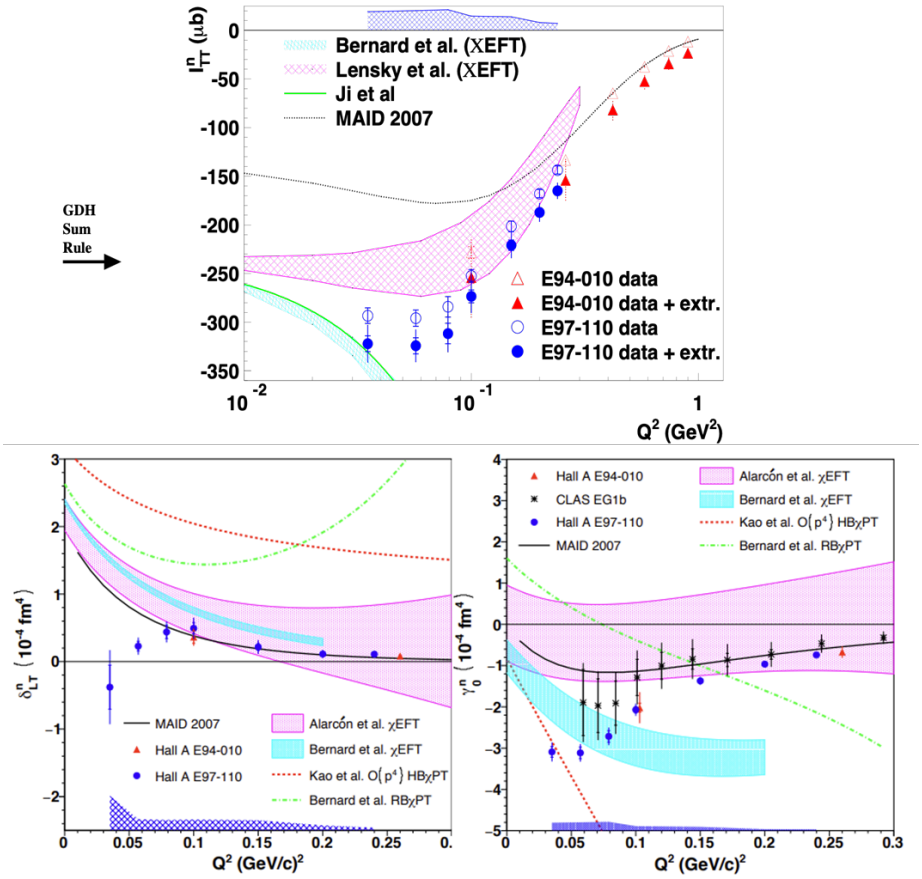

Figure 6: Moment results from the neutron data of E97110, including I_A (top), δ_{LT} (bottom left), and γ_0 (bottom right). [14]

the Alarcon et al. χPT calculation. Fully understanding this comparison to χPT however requires a full reconciliation of the two major calculations to understand all possible sources of tension.

2.5 EG4

The final experiment discussed here is a high precision measurement of the proton's longitudinal polarized cross section difference, or, an extraction of g_1 at very low Q^2. This experiment and E08-027, taken together, present a full picture of the proton's spin structure at low Q^2. EG4 ran in Hall B in 2006 with the CLAS detector, and utilized a specialized Cerenkov detector to improve efficiency at forward angles and enable very low Q^2 measurements. The experiment used a longitudinally polarized solid ammonia target to extract the proton's structure functions. The experiment also utilized deuterated ammonia (ND_3) for an additional extraction of the neutron and deuteron structure functions. EG4 published its first proton results in 2021 in *Nature Physics* [16]. The neutron results of EG4 are still under analysis at the time of this writing.

The proton results for the spin structure function moments from EG4 are shown in Figure 9. For most of the Q^2 range, the results agree best with the Alarcon et al. χPT calculation, but for each moment, the results cross into better agreement with the Bernard et al. calculation at the lowest Q^2. For I_A and Γ_1, the results also approach agreement with the GDH sum rule at low Q^2.

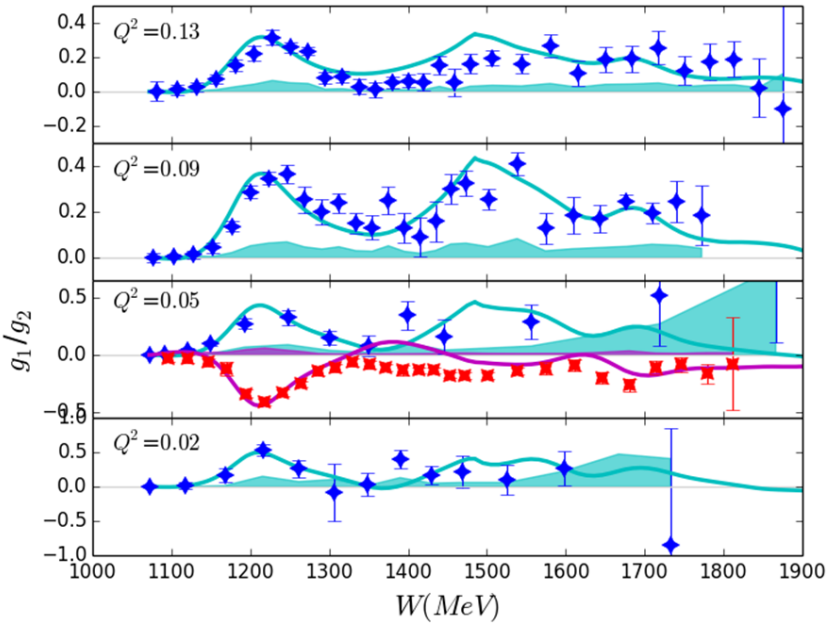

Figure 7: Structure function results from E08027. Blue + markers indicate g_2 results while Red x markers indicate the g_1 results. [15]

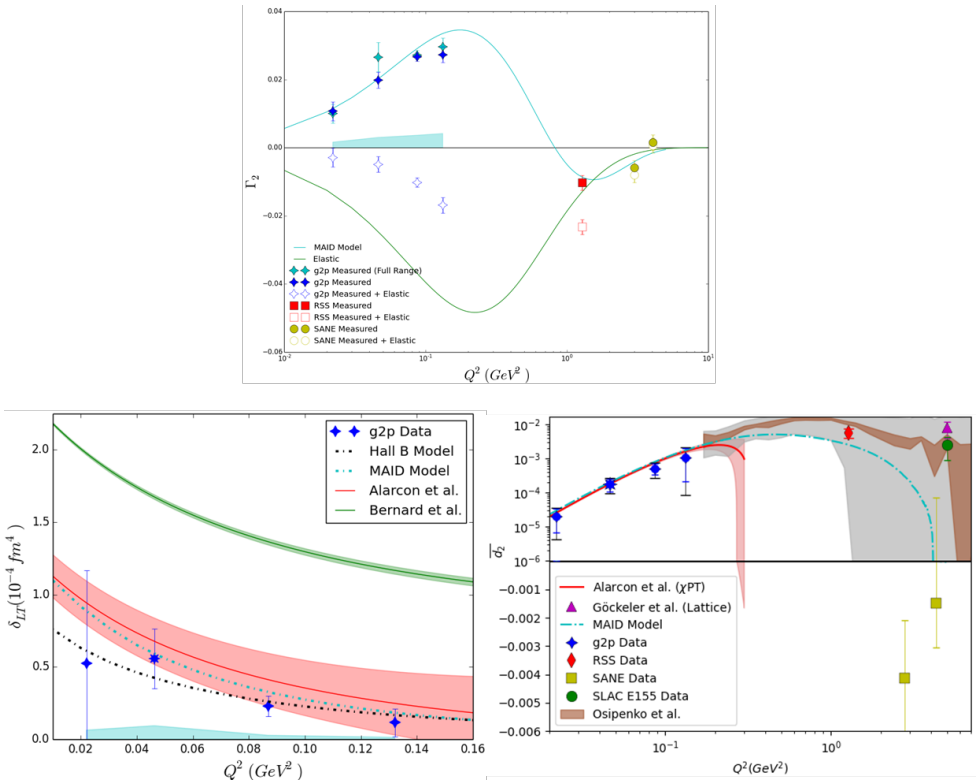

Figure 8: Moment results from the proton data of E08-027. The moments shown include Γ_2 (top), δ_{LT} (bottom left) and $\bar{d}_2$ (bottom right). [15]

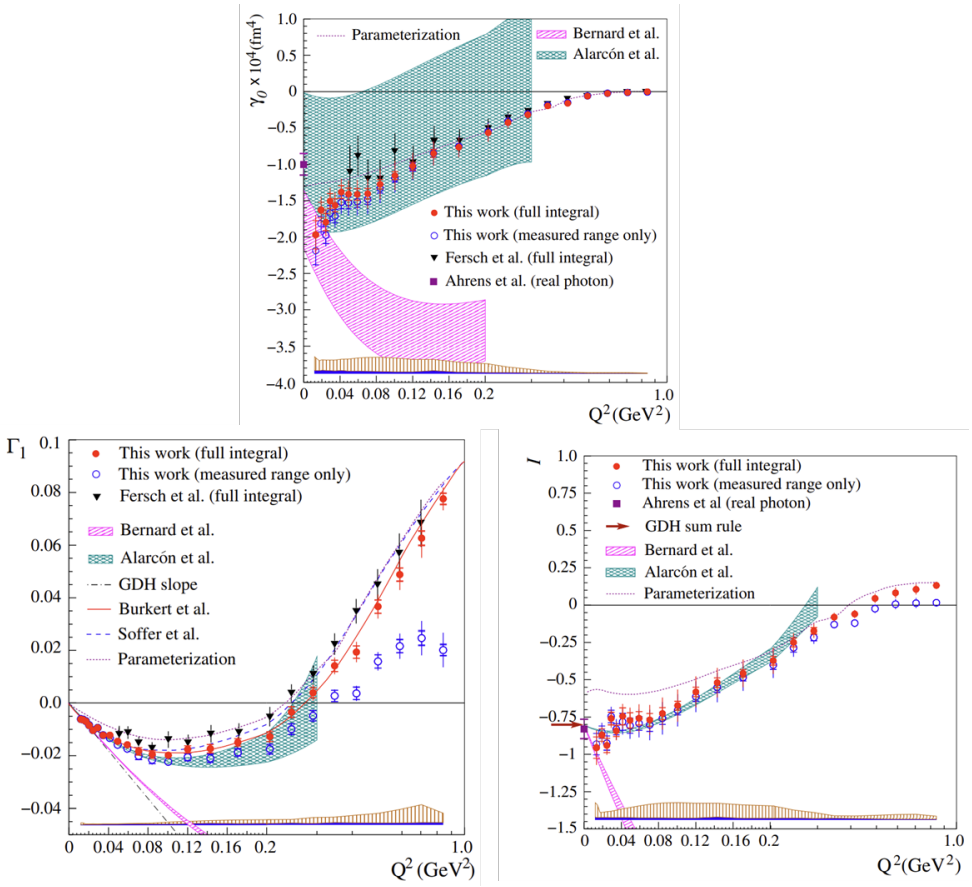

Figure 9: Proton moment results from EG4. Shown are γ_0 (top), Γ_1 (bottom left) and I_A (bottom right). [16]

2.6 Hydrogen Hyperfine Splitting

The principals of the E08-027 and EG4 experiments also collaborated to study another important quantity: the polarizability contribution to the hydrogen hyperfine splitting (HFS). This energy level splitting is one of the best-measured quantities in physics, but theoretical determinations of it are six orders of magnitude less precise due to a lack of knowledge about the proton structure, or polarizability, contribution. This polarizability contribution can be extracted with g_1 and g_2, but based on early determinations using a model of the structure functions at low Q^2, there was significant tension between the χPT determination of this contrubtion and experimental extractions of the same. As is shown in Figure 10, the new low Q^2 proton $g_{1,2}$ data from EG4 and E08-027 significantly reduces both the uncertainty and the tension on the data-driven extraction of the polarizability contribution to the HFS. This result was recently published in *Physics Letters B* [17].

3. Conclusion & Future Prospects

Measurements of the spin structure functions g_1 and g_2, as well as their moments, are a vital tool for benchmarking and testing low Q^2 effective theories such as chiral perturbation theory. Jefferson Lab in Newport News, VA has hosted a highly successful program measuring these structure functions for both nucleons over the last two decades, with several transformative low Q^2 extractions

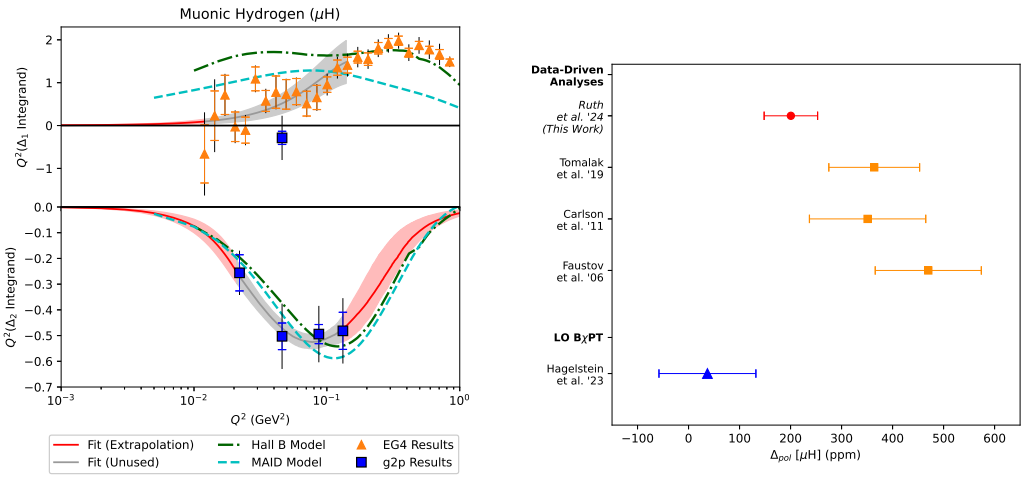

Figure 10: Results for the hyperfine splitting contributions Δ_1 and Δ_2 (left), see [17] for a full calculation of their combination. (right) Comparison for the polarizability HFS contribution Δ_{pol} between the new work (featuring EG4 and E08-027 data), older works which were driven by higher Q^2 data, and the result from χPT. [17]

being published in the last several years. There is significant experimental interest in continuing this JLab program: PR12-24-002 was conditionally approved with C2 status in 2024 to measure the proton's g_2 structure function in the transition region, mapping out the connection between the low Q^2 regime and the higher pQCD regime. Further understanding the sum rules and hyperfine splitting may also benefit from even lower Q^2 measurements of the spin structure functions, though due to the kinematics accessible at JLab, reaching 10^{-3} GeV^2 or lower may require other facilities or more creative solutions to access the very low Q^2 regime.

References

[1] D. Ruth. "A Strong-QCD Regime Measurement of the Proton's Spin Structure". PhD thesis. University of New Hampshire, 2022.

[2] A. W. Thomas and W. Weise. *The Structure of the Nucleon*. Berlin: Wiley, 2001. URL: https://cds.cern.ch/record/479090.

[3] M. Srednicki. *Quantum Field Theory*. Cambridge: Cambridge University Press, 2012.

[4] D. Drechsel. "Spin Sum Rules and Polarizabilities". In: *Spin Structure at Long Distance. Proceedings,Workshop, Newport News, USA, March 12-13, 2009*. Vol. 1155. 2009, pp. 3–17. DOI: 10.1063/1.3203300. arXiv: 0910.0719 [nucl-th].

[5] Jose Manuel Alarcón et al. "Forward doubly-virtual Compton scattering off the nucleon in chiral perturbation theory. II. Spin polarizabilities and moments of polarized structure functions". In: *Phys. Rev. D* 102 (11 Dec. 2020), p. 114026. DOI: 10.1103/PhysRevD.102.114026. URL: https://link.aps.org/doi/10.1103/PhysRevD.102.114026.

[6] D. Drechsel, B. Pasquini, and M. Vanderhaeghen. "Dispersion Relations in Real and Virtual Compton Scattering". In: *Phys. Rept.* 378 (2003), pp. 99–205. DOI: 10.1016/S0370-1573(02)00636-1. arXiv: hep-ph/0212124 [hep-ph].

[7] Robert L. Jaffe. "Spin, twist and hadron structure in deep inelastic processes". In: (1996). arXiv: hep-ph/9602236.

[8] J. Alcorn et al. "Basic Instrumentation for Hall A at Jefferson Lab". In: *Nucl. Instrum. Meth.* A522 (2004), pp. 294–346. DOI: 10.1016/j.nima.2003.11.415.

[9] J. Pierce, J. Maxwell, C. Keith, et al. "Dynamically Polarized target for the g2p and gep Experiments at Jefferson Lab". In: *Physics of Particles and Nuclei* 45.1 (2014), pp. 303–304. DOI: 10.1134/S1063779614010808. URL: http://dx.doi.org/10.1134/S1063779614010808.

[10] M. E. Christy and P. E. Bosted. "Empirical Fit to Precision Inclusive Electron–Proton Cross Sections in the Resonance region". In: *Phys. Rev. C* 81 (5 2010), p. 055213. DOI: 10.1103/PhysRevC.81.055213. URL: http://link.aps.org/doi/10.1103/PhysRevC.81.055213.

[11] M. Amarian et al. "Measurement of the Generalized Forward Spin Polarizabilities of the Neutron". In: *Phys. Rev. Lett.* 93 (15 2004), p. 152301. DOI: 10.1103/PhysRevLett.93.152301. URL: http://link.aps.org/doi/10.1103/PhysRevLett.93.152301.

[12] Robert Fersch et al. "Determination of the Proton Spin Structure Functions for $0.05 < Q^2 < 5$ GeV^2 using CLAS". In: *Phys. Rev. C* 96 (6 Dec. 2017), p. 065208. DOI: 10.1103/PhysRevC.96.065208. URL: https://link.aps.org/doi/10.1103/PhysRevC.96.065208.

[13] S. Wandzura and F. Wilczek. "Sum Rules for Spin-Dependent Electroproduction–Test of Relativistic Constituent Quarks". In: *Physics Letters B* 72.2 (1977), pp. 195–198. ISSN: 0370-2693. DOI: http://dx.doi.org/10.1016/0370-2693(77)90700-6. URL: http://www.sciencedirect.com/science/article/pii/0370269377907006.

[14] V. Sulkosky, C. Peng, J.P. Chen, et al. "Measurement of the generalized spin polarizabilities of the neutron in the low-Q2 region". In: *Nature Physics* 17 (2021), pp. 687–692. DOI: 10.1038/s41567-021-01245-9.

[15] D. Ruth, R. Zielinski, C. Gu, et al. "Proton spin structure and generalized polarizabilities in the strong quantum chromodynamics regime". In: *Nature Physics* 18 (2022), pp. 1441–1446. DOI: 10.1038/s41567-022-01781-y.

[16] X. Zheng, A. Deur, H. Kang, et al. "Measurement of the proton spin structure at long distances". In: *Nature Physics* 17 (2021), pp. 736–741. DOI: 10.1038/s41567-021-01198-z.

[17] David Ruth et al. "New spin structure constraints on hyperfine splitting and proton Zemach radius". In: *Physics Letters B* 859 (2024), p. 139116. ISSN: 0370-2693. DOI: https://doi.org/10.1016/j.physletb.2024.139116. URL: https://www.sciencedirect.com/science/article/pii/S0370269324006749.